MARY KAY O'CONNOR PROCESS SAFETY CENTER
TEXAS A&M ENGINEERING EXPERIMENT STATION

21st Annual International Symposium
October 23-25, 2018 | College Station, Texas

Transient Large-Scale Chlorine Releases in the Jack Rabbit II Field Tests: Estimates of the Airborne Mass Rate for Atmospheric Dispersion Modeling

Tom Spicer*
Ralph E. Martin Department of Chemical Engineering
University of Arkansas, Fayetteville, AR
+1.479.575.6516

Graham Tickle
GT Science & Software Ltd.
Chester, UK

*Corresponding author: tos@uark.edu

Abstract

Sponsored by the U.S. Department of Homeland Security, the Defense Threat Reduction Agency (DTRA) of the U.S. Department of Defense, and Transport Canada, the Jack Rabbit II tests were designed to release liquid chlorine at ambient temperature in quantities of 5 to 20 T for the purpose of quantifying the behavior and hazards of catastrophic chlorine releases at scales represented by rail and truck transport vessels. In 2015, five successful field trials were conducted in which chlorine was released in quantities of 5 to 10 tons through a 6-inch circular breach in the tank and directed vertically downward at 1 m elevation over a concrete pad. In 2016, three additional trials were conducted with releases of 10 tons also through 6-inch circular breaches at different release orientations. A final 20 ton test was conducted in 2016. Data from the test program is available. This paper summarizes assessment of the chlorine rainout and provides estimates of the mass of chlorine moving with the wind field as a function of time.

Introduction

Sponsored by the U.S. Department of Homeland Security, the Defense Threat Reduction Agency (DTRA) of the U.S. Department of Defense, and Transport Canada, the Jack Rabbit II tests were designed to release liquid chlorine at ambient temperature in quantities of 5 to 20 T for the purpose of quantifying the behavior and hazards of catastrophic chlorine releases at scales represented by rail and truck transport vessels. In 2015, five successful field trials were conducted in which chlorine was released in quantities of 5 to 10 tons through a 6-inch circular breach in the tank and directed vertically downward at 1 m elevation over a concrete pad. In

2016, three additional trials were conducted with releases of 10 tons also through 6-inch circular breaches at different release orientations. A final 20 ton test was conducted in 2016. Data from the test program is available.

There are ongoing efforts to analyze data from the test program. One aspect of this analysis involves comparison of selected tests with predictions using available atmospheric dispersion models. For this comparison between atmospheric dispersion models to be most meaningful, it was desired to have a common set of model inputs including meteorological parameters and source parameters. This work represents the effort to prepare representative source parameters that can be applied in many different atmospheric dispersion models. Sections 1-5 below are summaries of previous work that analyze the test data (Spicer and Miller, 2018, and Spicer et al., 2018). Sections 6 and 7 discuss the extension of the present analysis to provide inputs for dispersion models used in the comparison exercise.

1. Liquid Volume as a function of Liquid Depth in the Disseminator

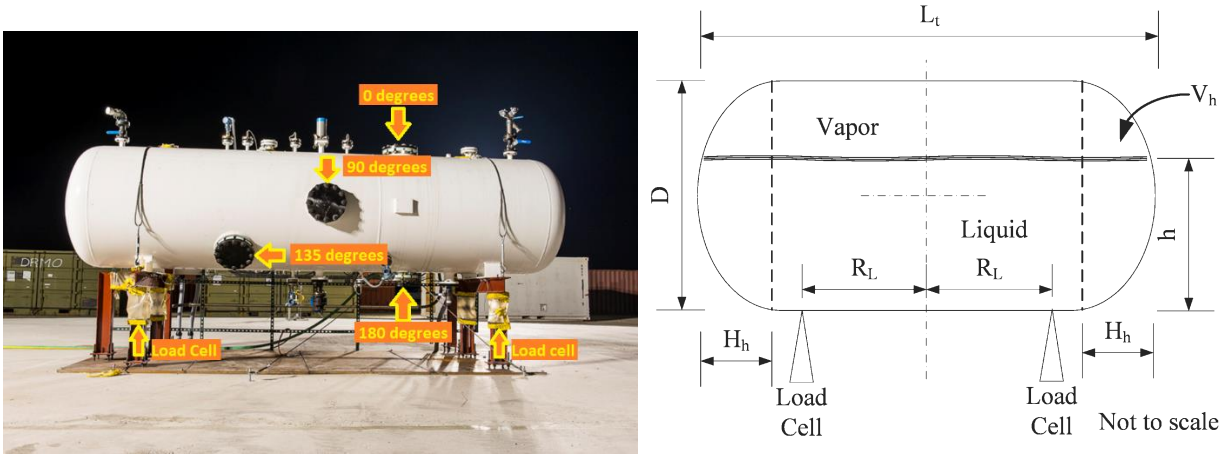

Figure 1. (a) Dissemination vessel on the 25 m concrete pad. (b) Schematic of the disseminator defining parameters.

The liquid volume (V_L) as a function of liquid depth in the vessel was calculated based on formulas (Couper et al., 2005) as follows,

$$V_h = \frac{\pi}{24} D^3 \tag{1}$$

$$V_L = (L_t - 2H_h)\left[\left(h - \frac{D}{2}\right)(Dh - h^2)^{1/2} + \left(\frac{D}{2}\right)^2 \cos^{-1}\left(\frac{D - 2h}{D}\right)\right] + 2\,V_h \left(\frac{h}{D}\right)^2 \left(3 - \frac{2h}{D}\right) \tag{2}$$

where h is the liquid depth and D is the inner diameter of the cylindrical vessel, respectively (Figure 1b). The volume of one head is V_h, and the depth of each head is H_h (both quantities excluding the straight flange), so the length of the cylindrical middle is $L_t - 2\ H_h$ where L_t is the tangent-to-tangent internal tank length. For a 2:1 semi-elliptical head as specified for the dissemination vessel used here, the volume V_h of a single head is given by the formula above, and the head depth H_h is D/4. As written above, the formula for V_L is suitable for all values of h including the full volume (h = D). Using a tangent-to-tangent internal length of 5.61 m (221 in) and inside diameter of 1.35 m (53.1 in) with a uniform shell thickness of 12.7 mm (0.5 in), the calculated vessel capacity is 7.70 m^3 (2034 gal). DPG measured the volume of the disseminator by filling it with a metered quantity of water and found the volume to be 7.65 m^3 (2020 gal). In the calculations that follow, a volume of 7.70 m^3 (2034 gal) will be used for the vessel volume.
.

2. Dynamic mass and thrust measurements

The load cell measurements provided the most consistent measurement of mass in the vessel under static conditions, and the load cell measurements can also be analyzed as a function of time. The vertical release ports were positioned with a moment arm away from the center of mass of the tank and its contents to determine dynamic mass separately from the release thrust. From a position facing into the (historic) mean wind direction and also facing the tank (consistent with the orientation in Figure 1), the load cells were designated as front (north side), back (south side), right (west side), and left (east side). The vertical release ports (0° and 180°) were located on the right (west side) centered 0.94 m (37 in) from the axial tank center (center of mass), and the 135° release port was located on the left (east side) side also centered 0.94 m (37 in) from the axial tank center. The horizontal release port (90°) was located on the axial tank center (but never used due to program limits).

Assuming any load cell deflection changes were small during the release, the sum of the vertical forces and torques (about the center of mass) are zero:

$$\sum F_z = 0 = Mg - d_m T_z - (\sum F_E + \sum F_W) \tag{3}$$

$$\sum \tau = 0 = T_z R_T + d_t(\sum F_W R_L - \sum F_E R_L) \tag{4}$$

where M is the mass of chlorine in the vessel, g is the acceleration due to gravity, T_z is the vertical thrust due to the jet release with moment arm R_T (0.94 m or 37 in), F_E and F_W are the load cell forces on east and west ends, respectively, with moment arm R_L (1.91 m or 75 in; see Figure 1b), and d_m and d_t are constants reflecting the release direction. d_t is chosen so that all thrust values are positive (-1 for 0° and 135° releases since those ports would create a clockwise rotation of the disseminator and +1 for 180° releases which would create a counter-clockwise rotation of the disseminator as pictured in Figure 1), and d_m reflects whether the thrust increases the load cell measurements (-1 for the 0° release since this force acts downward and +1 otherwise since these forces act upward). Equation 4 does not account for the vertical change of the center of mass as the vessel empties (which has been shown to result in small changes in liquid level along the axis of the disseminator). Also, the downward force due to atmospheric pressure on the top of the vessel opposite the jet is ignored. The load cell forces were tared with

measurements after the release was complete. The vertical thrust is found from Equation 4, and the chlorine mass from Equation 3. (The load cells measuring horizontal forces were not analyzed here.) There was some scatter associated with the processed data as was anticipated (particularly at the start of the release). In addition to the data acquisition system failure during Trial 5, load cell recorded values between (roughly) 38:59 and 39:02 during Trial 4 did not change indicating additional data acquisition problems. In Trial 6, data from the improved acquisition system show a sinusoidal variation which likely reflects (axial) liquid level variation in the disseminator (sloshing).

To determine the (essentially constant) average initial release rate, an averaging time period was used. The start of the time period was taken to be the last set of recorded values before the release, and the end of the time period was chosen to match the slope of the recorded mass as a function of time. The mass rate was calculated as the difference in mass between the beginning and end of the time period divided by the time period so that the derived values will match the mass remaining in the vessel. Table 1 summarizes these initial (constant) mass rates ($\dot{M}_i$) and the averaging time period.

Table 1. Jack Rabbit II Mass Release Parameters

Trial	Initial Mass (kg)	Initial Rate (kg/s)	Averaging Time for Initial Rate (s)	Inventory after Initial Rate (M_x) at Time t_x (kg @ s)	Time Constant τ_x (s)	Power p	Heel (kg)	Data Rate (Hz)
1	4,545	224	14	1,524 @ 13.5	6.80	1	0	1
2	8,192	273	23.4	1,968 @ 22.8	7.20	1	0	10
3	4,568	275	11.3	1,988 @ 9.39	7.24	1	0	10
4	7,017	271	20.7	1,784 @ 19.3	6.59	1	0	10
5	8,346	not available					0	10
6	8,391	260	24.9	1,779 @ 25.4	6.83	1	0	25
7	9,072	259	23.9	3,175 @ 22.7	10.5	1	446	25
8	9,120	170	3.12	8,591 @ 3.12	23.9	0.867	6,698	25
9	17,700	not available						

The time period when the initial mass release rate ($\dot{M}_x$) was (approximately) constant was followed by a period when the rate steadily declined. While the mass rate could be obtained directly from the data during this later period, this would be cumbersome in practice, so this interval was fit using standard least squares to:

$$(M - M_h) = (M_x - M_h)\, exp\left(-\left(\frac{t - t_x}{\tau_x}\right)^p\right) \quad (5)$$

where M_x is the inventory at time t_x, M_h is the release heel, and τ_x and p are parameters determined in the fitting process (in Trials 1-4, 6, and 7, p = 1 proved a sufficient fit of the data). Equation 5 can be differentiated to determine the mass rate as a function of time (as long as $p \geq 1$), but this rate so determined could create a discontinuity at time t_x with $\dot{M}_x$ because $M_x = M_i - \dot{M}_x t_x$ where M_i is the initial disseminator inventory. This issue can resolved by simultaneously fitting t_x and τ_x to the data using the values for $\dot{M}_x$ as obtained previously. Table 1 includes data obtained for all trials. It is important to note that the integrated dynamic mass measurements were consistent with (static) mass measurements before and after the release.

For Trial 7, the release port chosen was 45° below horizontal, and consequently, mass remained in the vessel (heel in Table 1) after the first (primary) release. As in the previous trials, the end of the primary release was modeled using Equation 5 up to t = 84.1 s when the remaining heel was slowly releasing chlorine due to heat transfer to the remaining (subcooled) liquid. The heel was taken to be the average chlorine mass remaining in the disseminator measured between 84.1 and 94.1 s. The remaining heel was dumped from the disseminator using a remotely operated valve at 11:07.43 (after the primary release was deemed to be complete at the time of testing). It is worth noting that the maximum amount of chlorine that could remain in the vessel after a release from this orientation is 686 kg (i.e., the potential inventory when the liquid level would be at the same elevation as the bottom of the release opening), and since only 446 kg (65%) was measured to remain, 35% of the potential inventory actually flashed during the primary release. Video records indicate that the chlorine leaving the disseminator at the end of the test was flashing as opposed to simply being pushed out of the vessel by liquid swell.

In Trial 8, the release was vertically upward with significant mass remaining in the vessel after the primary release. During the initial phases of the release, a vapor (only) release would be expected since the opening was in the vapor space. Based on choked ideal gas flow at the storage conditions, the mass release rate is predicted to be 39 kg/s, and prior to the release, the vapor space was 1.30 m^3, so the vapor space would have been emptied in about 0.6 s. In the video record, the initial speed of the release clearly decreases after about 0.6 s and becomes stable at around 2.4 s. The load cell data seemed to be more consistent after 3.12 s (slightly later than video observations), so the initial phase of the release (first 3.12 s) was modeled assuming a constant release rate. As in the previous trials, the end of the primary release was modeled using Equation 5 (with p = 0.867) up to t = 100 s when the remaining heel was slowly releasing chlorine due to heat transfer to the remaining (subcooled) liquid. The heel was taken to be the average chlorine mass remaining in the disseminator measured between 90 and 100 s. (Since $p<1$, $\dot{M}$ cannot be calculated at t_i using Equation 5, but a simple approximation would be to assume the constant rate $\dot{M}_i$ applies up to 3.146 s where Equation 5 can be differentiated and would be the same mass rate.) As in Trial 7, the remaining heel was dumped from the

disseminator using a remotely operated valve at 15:30.53. In Trial 8, the maximum amount of chlorine that could remain in the vessel after a release from this orientation was the tank inventory (in this case 9,122 kg); 6,698 kg (73%) was measured to remain, and consequently, 27% of the potential inventory actually flashed during the primary release.

3. Time Varying Mass Release Rate

As discussed above, the time period when the initial mass release rate ($\dot{M}_x$) was (approximately) constant was followed by a period when the rate steadily declined. Equation 5 can be differentiated to find the mass release rate (-dM/dt) as a function of time after t_x:

$$\left(-\frac{dM}{dt}\right) = \frac{(M_x - M_h)}{\tau_x}\, exp\left(-\left(\frac{t-t_x}{\tau_x}\right)^p\right) p \left(\frac{t - t_x}{\tau_x}\right)^{p-1} \tag{6}$$

which reduces to

$$\left(-\frac{dM}{dt}\right) = \frac{(M_x - M_h)}{\tau_x}\, exp\left(-\left(\frac{t-t_x}{\tau_x}\right)\right) \tag{7}$$

when p = 1 (in Trials 1-4, 6, and 7). To summarize, the mass release rate ($\dot{M}_R$) is given by:

$$\begin{aligned} \dot{M}_R &= \dot{M}_x && for\ t \le t_x \\ &= \left(-\frac{dM}{dt}\right) && for\ t > t_x \end{aligned} \tag{8}$$

where -dM/dt is given by Equations 6 or 7. Note that Equation 7 should be used for all trials except Trial 8.

4. Impact of Rainout and Subsequent Re-Evaporation

Temperature measurements from the 2015 test season indicated the liquid that rained out formed thin liquid puddles that evaporated while remaining at the liquid chlorine boiling point. There were indications that the force of the release pushed liquid that rained out toward the periphery of the pad (surface temperatures at Pad 2 near the release were consistent with direct exposure to the aerosol because the measured temperature was significantly colder than the chlorine boiling point).

Video recordings in the 2016 test season were less obstructed and provided an opportunity in Trial 6 to determine the area coverage of the liquid. Trial 6 is also worthwhile to study because the infrared video shows that the liquid was contained on the concrete pad (some potential, limited overflow to the gravel is indicated on the IR images). During the initial phase of the release from containment, the aerosol cloud effectively shields the rained out liquid from solar radiation or heating by the air, so the majority of heat transfer to the liquid is by conduction from the concrete pad (effectively modeled by conduction in a semi-infinite solid with a constant

surface temperature boundary condition). The IR video was not used because cold concrete cannot be easily distinguished from concrete covered by liquid.

The following assumptions are used in this analysis:

1. The total deposition is equal to the total mass evaporated by thermal conduction from the concrete slab.
2. Because the deposition process is driven by the primary release from containment, assume the deposition rate is proportional to the release rate over the duration of the deposition.
3. Heat conduction from the slab will exceed the deposition rate initially, but after a brief period ($t = t_e$), the rate of evaporation will be controlled by the rate of heat conduction from the concrete pad.
4. The time when deposition/rainout ends (t_d) must presently be determined from the video record. For Trial 6, the jet angle changes at about 38.83 s, but the color of the jet is unchanged (indicating the presence of aerosol continues). At 48.2 s, the color of the jet changes in a manner consistent with the initial phase of Trial 8 when the release begins as a vapor but makes the transition to aerosol, and this would correspond to $t_d = t_x + 3.34\tau_x$. Video from the other trials showed a similar transition ranging from $t_d = t_x + 3.09\tau_x$ (Trial 1) to $t_d = t_x + 3.56\tau_x$ (Trial 2). Based on the average of the vertically downward jet releases, assume that $t_d = t_x + 3.4\tau_x$. The transition seems to occur at a later time in Trial 7, so for this trial, $t_d = t_x + 3.7\tau_x$.
5. The concrete pad seems fully wetted (covered by liquid) up to $t_w = 41.4$ s as indicated by visible video frames when the first dry concrete can be observed. After 41.4 s, the area covered by liquid is observed to decrease in regions where the pad can be observed. The view of the concrete pad is unobstructed by vapor puffs after 50.2 s. (Assuming complete coverage by the liquid will tend to overestimate the evaporation because the Pad 2 temperature measurements from 2015 indicated that there was likely no liquid coverage near the release point caused by the force of the release. This region is also partially obscured at 41.4 s in the visible video. Pad 2 is at a radius of 4 m from the release, and if the area inside a radius of 4 m was not covered, this would represent 10% of the concrete pad area or a coverage of 0.9.) Based on the observations above, $t_w \approx t_x + 2.35\tau_x$.

To summarize, the evaporation rate is equal to the deposition rate from $t = 0$ to t_e. From $t = t_e$ to t_w, liquid covers a large portion of the concrete pad surface, and this area coverage is assumed to be approximately constant. After $t = t_w$, the visible area of the liquid covering the pad decreases in time until the last puddle has evaporated. Deposition occurs up to $t = t_d$. Based on the video record, the visible area of liquid covering the pad begins to decrease before the deposition is complete.

Under a constant surface temperature boundary condition, the heat flux from a solid can be calculated using Fourier's law

$$q''(t) = \frac{k\,\Delta T}{\sqrt{\pi\,\alpha\,t}} \tag{9}$$

where the temperature difference ΔT is $T_p - T_o$, and T_p is the pad temperature. The pad temperature was estimated from the average temperature over the 1 minute interval prior to the release at 3 mm below grade averaged over all three pad locations (provided data was available except Trial 1 when the measurements at 6 mm below grade were used since the 3 mm measurements were not available). Pad temperatures were 19.8 C, 24.2 C, 22.4 C, 22.4 C, 22.4 C, 22.9 C, 19.4 C, and 16.7 C for Trials 1-8, respectively. Provided that the area covered by liquid chlorine can be quantified as a function of time A(t), the total amount of heat transferred from the concrete Q(t) at time t is given by:

$$Q(t) = \int_0^t q''(t)\, A(t)\, dt = \int_0^t \frac{k\,\Delta T}{\sqrt{\pi\,\alpha\,t}}\, A(t)\, dt \qquad (10$$

Consequently, the total mass evolved or evaporated from the surface $M_e(t)$ is given by:

$$M_e(t) = \frac{k\,\Delta T}{\Delta H_v} \int_0^t \frac{A(t)}{\sqrt{\pi\,\alpha\,t}}\, dt \qquad (11$$

Based on the visible video analysis, the concrete pad area fraction covered by liquid is shown in Figure 2. The solid line indicates a best fit to an exponential decay (with time constant τ_e):

$$\begin{aligned} A(t) &= f_{a,0} A_p && 0 \le t \le t_w \\ &= f_{a,0} A_p e^{-(t - t_w)/\tau_w} && t > t_w \end{aligned} \qquad (12)$$

where $f_{a,o}$ is the initial fraction of pad area covered by liquid and A_p is the area of the concrete pad. As indicated in the figure, a value of $f_{a,o}$ = 0.9 fits the data well (τ_w = 297 s).

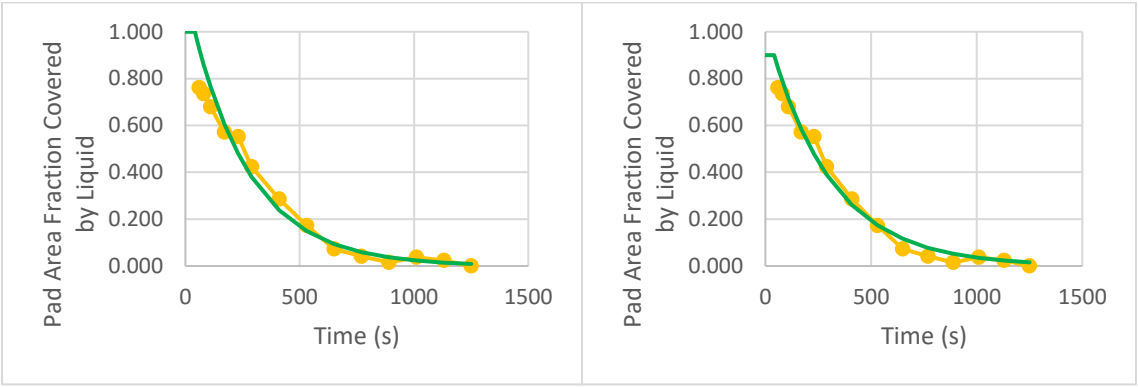

Figure 2. Liquid coverage of concrete pad as a function of time: (a) $f_{a,o}$ = 1; (b) $f_{a,o}$ = 0.9.

Equation 11 provides an estimate of the mass evaporated from t = 0, but the evaporation rate obtained from differentiating Equation 11 will be infinite at t = 0 (consistent with q" being infinite at t = 0). As discussed above, the evaporation rate is limited by the deposition rate for $t \le t_e$. Consequently, the time used to model the heat conduction rate from the concrete cannot

correspond to the start of the release (t = 0) to account for this (physical) limit. Define t_o as the initial time to be used in Fourier's Law model to account for this limitation; t_o is chosen so that the total deposition at t_e is equal to the total mass evolved by heat transfer at ($t_e - t_o$) and the deposition rate at t_e is equal to rate mass is evolved by heat transfer at ($t_e - t_o$). Considering the time when the deposition rate is equal to the evaporation rate (t_e), Equation 11 becomes

$$M_e(t_e) = \frac{k\,\Delta T}{\Delta H_v}\int_{t_o}^{t_e}\frac{f_{a,o}A_p}{\sqrt{\pi\,\alpha\,(t\,-\,t_o)}}\,dt = \frac{k\,\Delta T}{\Delta H_v}\int_{0}^{t_e\,-\,t_o}\frac{f_{a,o}A_p}{\sqrt{\pi\,\alpha\,t}}\,dt = \frac{k\,\Delta T}{\Delta H_v}\left[2f_{a,o}A_p\sqrt{\frac{(t_e\,-\,t_o)}{\pi\,\alpha}}\right] = t_e\dot{M}_d(t_e) \quad (1$$

where $\dot{M}_d$ is the deposition rate (initially constant when the release rate is constant). Also, Equation 9 is related to the deposition rate by:

$$\dot{M}_d(t_e) = \frac{k\,\Delta T\,f_{a,o}A_p}{\Delta H_v\sqrt{\pi\,\alpha\,(t_e\,-\,t_o)}} \quad (14$$

Equations 13 and 14 can be solved simultaneously to determine that $t_o = t_e/2$, and values for all of the parameters can be determined once $\dot{M}_d$ is found. (Values of t_e were less than 2 s for scenarios considered below.)

When the last puddle of liquid chlorine has evaporated, the total rainout from the release can then be determined. Using the area covered by liquid, Equation (13) becomes:

$$M_e(t) = \frac{k\,\Delta T}{\Delta H_v}\left[\int_0^{t_w\,-\,t_o}\frac{f_{a,o}A_p}{\sqrt{\pi\,\alpha\,t}}\,dt + \int_{t_w\,-\,t_o}^{t\,-\,t_o}\frac{f_{a,o}A_p e^{-(t+t_o-t_w)/\tau_w}}{\sqrt{\pi\,\alpha\,t}}\,dt\right] = \frac{k\,\Delta T}{\Delta H_v}\left[2f_{a,o}A_p\sqrt{\frac{(t_w\,-\,t_o)}{\pi\,\alpha}}\right]\left[1 + \frac{\sqrt{\pi}}{2}\left(\frac{\tau_w}{t_w\,-\,t_o}\right)^{1/2}e^{+(t_w-t_o)/\tau_w}\left(erf\left(\left(\frac{t\,-\,t_o}{\tau_w}\right)^{1/2}\right) - erf\left(\left(\frac{t_w\,-\,t_o}{\tau_w}\right)^{1/2}\right)\right)\right] \quad (15$$

As discussed above, there are uncertainties in the evaluation of $f_{a,o}$, and this uncertainty influences the value for τ_w based on a curve fit of the data. In the fitting process, τ_w increases as $f_{a,o}$ decreases; these effects can be seen by considering the right hand side of Equation (15):

$$M_e(t) \propto f_{a,o}\left[1 + \frac{\sqrt{\pi}}{2}\left(\frac{\tau_w}{t_w - t_o}\right)^{1/2} e^{+(t_w - t_o)/\tau_w}\left(erf\left(\left(\frac{t - t_o}{\tau_w}\right)^{1/2}\right) - erf\left(\left(\frac{t_w - t_o}{\tau_w}\right)^{1/2}\right)\right)\right] \quad (16)$$

As $f_{a,o}$ decreases, the term inside the brackets increases because of the increase in τ_w. For $f_{a,o}$ ranging from 0.9 to 1.0, the right hand side of Equation (12) ranges from 2.40 to 2.50, respectively (roughly 5% change) evaluated for the time when the last puddle has evaporated.

Using generic properties for the concrete pad, the temperature difference between chlorine at its (local) boiling point and ambient temperature, and a heat of vaporization of 2.897×10^{-5} J/kg, the total mass evaporated (M_e) for Trial 6 is estimated to be 2938 kg. As discussed above, the total mass evaporated is also the total deposited or rained out ($M_d = M_e$). The initial mass in the vessel was 8391 kg, so the mass rained out represents approximately 35% of the mass released. Previous CCPS tests using chlorine that attempted to directly measure liquid rainout found the rainout to be roughly 17% of the released mass for a horizontal release at 1.22 m elevation (D.W. Johnson, and J.L. Woodward, "RELEASE-A model with Data to Predict Aerosol Rainout in Accidental Releases," AIChE CCPS, 1999).

With the total mass deposited (rained out), M_d, estimated above, the deposition rate can be determined based on the assumption that the deposition rate is proportional to the release rate. If the deposition ends at $t = t_d$, the mass deposited is given by

$$M_d(t) = \left(\frac{M_d}{M_r(t_d)}\right) M_r(t) \quad (17)$$

where $M_r(t_d)$ is evaluated as

$$M_r(t_d) = \dot{M}_x t_x + (M_x - M_h)\left[1 - exp\left(-\left(\frac{t_d - t_x}{\tau_x}\right)\right)\right] \quad (18)$$

The mass deposition rate ($\dot{M}_d$) is given by:

$$\dot{M}_d = \left(\frac{M_d}{M_r(t_d)}\right)\dot{M}_x(t) \qquad t \le t_x$$
$$= \left(\frac{M_d}{M_r(t_d)}\right)\frac{(M_x - M_h)}{\tau_x}\, exp\left(-\left(\frac{t - t_x}{\tau_x}\right)\right) \qquad t > t_x \quad (19)$$

With the deposition rate determined, the evaporation rate can be calculated using

$$\dot{M}_e = \dot{M}_d \qquad t \le t_e$$
$$= \frac{k\,\Delta T\, f_{a,o} A_p}{\Delta H_v \sqrt{\pi\,\alpha\,(t - t_o)}} \qquad t_e < t \le t_w$$
$$= \frac{k\,\Delta T\, f_{a,o} A_p}{\Delta H_v \sqrt{\pi\,\alpha\,(t - t_o)}}\, exp\left(-\left(\frac{t - t_w}{\tau_w}\right)\right) \qquad t > t_w \qquad (20$$

5. Airborne Chlorine Mass Rate for Trial 6

The mass rate chlorine becomes airborne $\dot{M}_a$is estimated using

$$\dot{M}_a(t) = \dot{M}_r(t) - \dot{M}_d(t) + \dot{M}_e(t) \qquad (21$$

Note that the deposition occurs from the liquid phase while evaporation contributes to the vapor phase only so that the liquid fraction of the airborne aerosol is changed by these processes. Figure 3 summarizes the result for Trial 6. For this calculation, the mass release rate is taken to be zero when the calculated rate drops below 1 kg/s (at 63.4 s). (The mass release rate is modeled with an exponential decay, so it would continue long after its contribution was negligible without a criterion for it to stop.) The same approach to estimating the rainout rate and duration can be applied to Trials 1-7, provided the rainout percentage is assumed constant since the release rates are comparable across Trials 1-7. In Trial 6, the last puddle evaporated at 1250 s with a corresponding estimated evaporation rate of 0.042 kg/s, and this ending rate will be used in the analysis of the other trials.

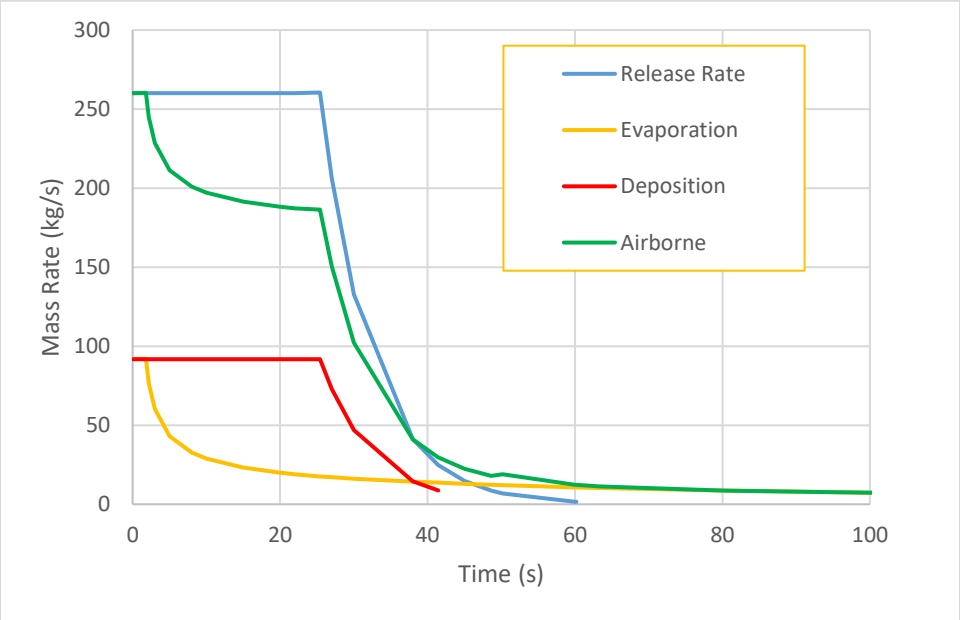

Figure 3. Instantaneous airborne mass rate as a function of time for Trial 6.

Figure 3 makes clear that the mass rate is consistently high for times less than t_x. At t_x, $M_r(t_x)$ = 6612 kg, $M_d(t_x)$ = 2333 kg, and $M_e(t_x)$ = 864, so the total mass airborne would be 5143 kg, so the average airborne mass rate would be 5143 kg/25.4 s = 202 kg/s. For times larger than t_x, the time varying airborne mass rate drops off rapidly. Note that the calculated (instantaneous) mass airborne rate is not monotonically decreasing at the time that deposition ends because the deposition rate is not continuous at t_d.

As an alternate approach, the average airborne rate can be calculated from the (total) cumulative airborne mass divided by the time over which that mass becomes airborne. Figure 4 shows the cumulative airborne mass and average airborne mass rate as a function of time. In addition to the total cumulative mass released, deposited, and evaporated, Table 2 includes average airborne mass rates for various times. The average vapor fraction in Table 2 is the total airborne vapor mass up to time t divided by the total airborne mass at the same time. The average vapor fraction is a strong function of the (adiabatic) flash fraction from storage conditions which was calculated for the (local) boiling point ignoring kinetic energy effects. The flash fraction was assumed constant until t_d and 1 thereafter (all mass released directly to the vapor phase). The final time in Table 2 of 63.4 s was chosen when the mass release rate drops below 1 kg/s, which is taken to be the time the (vapor only) jet has ended.

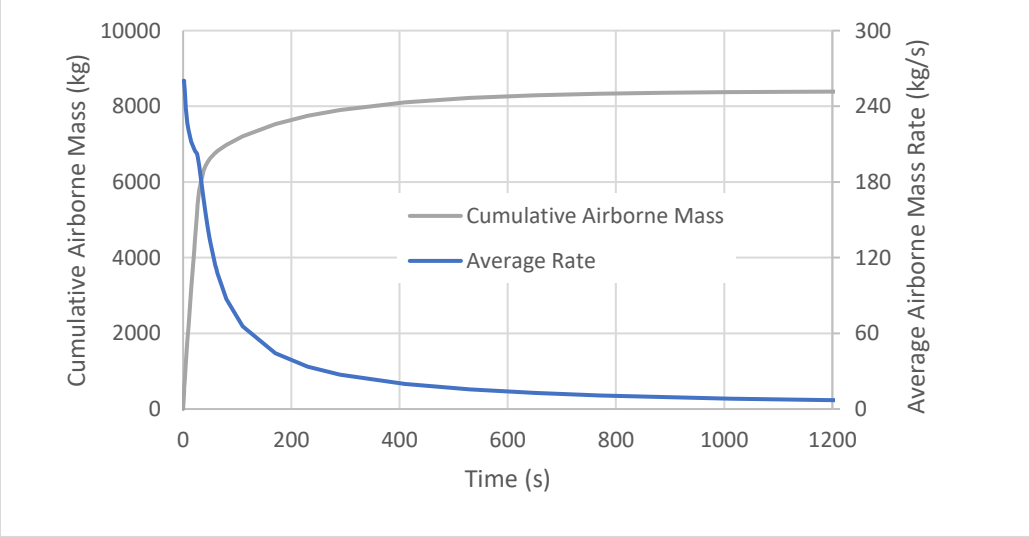

Figure 4. Cumulative airborne mass and average airborne rate as a function of time for Trial 6

Table 2. Cumulative mass fate and average airborne mass rate as a function of time for Trial 6.

Time, t (s)	Mass Released by t (kg)	Mass Deposited by t (kg)	Mass Airborne from Primary Release by t (kg)	Mass Evaporated by t (kg)	Average Vapor Fraction	Average Airborne Mass Rate (kg/s)
20	5200	1835	3365	763	0.401	206
25.4 (t_x)	6612	2334	4278	864	0.389	202
30	7484	2641	4843	942	0.385	193
48.6 (t_d)	8332	2938	5394	1205	0.400	136
60	8380	2938	5442	1335	0.416	113
63.4	8384	2938	5447	1371	0.420	108

6. Airborne Chlorine Mass Rate for Trials 1, 6, and 7

The approach developed to analyze Trial 6 was applied to Trials 1 and 7. To summarize the process,

1. The mass release parameters were determined as discussed above:
    a. The total mass released was determined from load cell data in conjunction with the liquid heel remaining after the release. (The heel was determined for Trials 7 and 8 to be the point when the change in mass readings was less than 1 kg from the average reading for at least 1 s.)
    b. The start of the release (t=0) was the last set of recorded values before they significantly changed. The initial average mass rate was calculated as the difference in mass between the beginning and end of the averaging time period divided by the averaging time period so that the derived values will match the mass remaining in the vessel. The length of the time period was limited to when the rate was no longer essentially constant.
    c. The parameters M_x, t_x, and τ_x were determined from the measured mass as a function of time so that the mass release rate was continuous at t_x (transition from continuous release rate to release rate decreasing with time at the end of the release).
    d. The parameters t_d (= $t_x + 3.4\tau_x$) and t_w (= $t_x + 2.35\tau_x$) from Trial 6 were assumed to apply to the other trials except Trial 7 where $t_d = t_x + 3.7\tau_x$.
2. The chlorine boiling point (used in the driving force for heat transfer to the concrete pad) was obtained at the reported ambient pressure at the time of the release using the vapor pressure correlation for chlorine from DIPPR. Average pad temperatures were found as discussed above.

3. The chlorine initial flash fraction was estimated assuming an isenthalpic flash to ambient temperature using the latent heat of vaporization correlation for chlorine from DIPPR and (mean) liquid heat capacity correlated from Chlorine Institute Pamphlet 72.
4. The initial fraction of pad area covered by the liquid and the rain out fraction were assumed constant for Trials 1-7 based on the analysis of Trial 6 discussed above.

The results for Trials 1 and 7 are shown in Figures 5 and 6 and Tables 3 and 4, respectively. This approach predicts that the last puddle of liquid evaporates at 380 s on Trial 1 and 1600 s on Trial 7. In Trial 1, there are several small puddles still visible at 380 s. In Trial 7, the liquid clearly deposited outside the concrete pad on the gravel surrounding the pad, and at 1600 s, the gravel is white indicating the presence of condensed and frozen water.

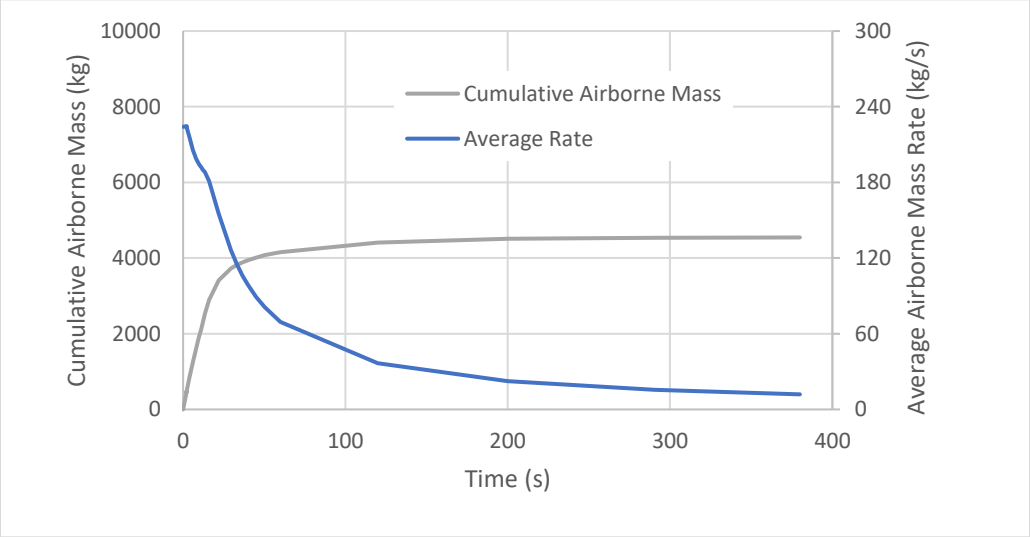

Figure 5. Cumulative airborne mass and average airborne rate as a function of time for Trial 1.

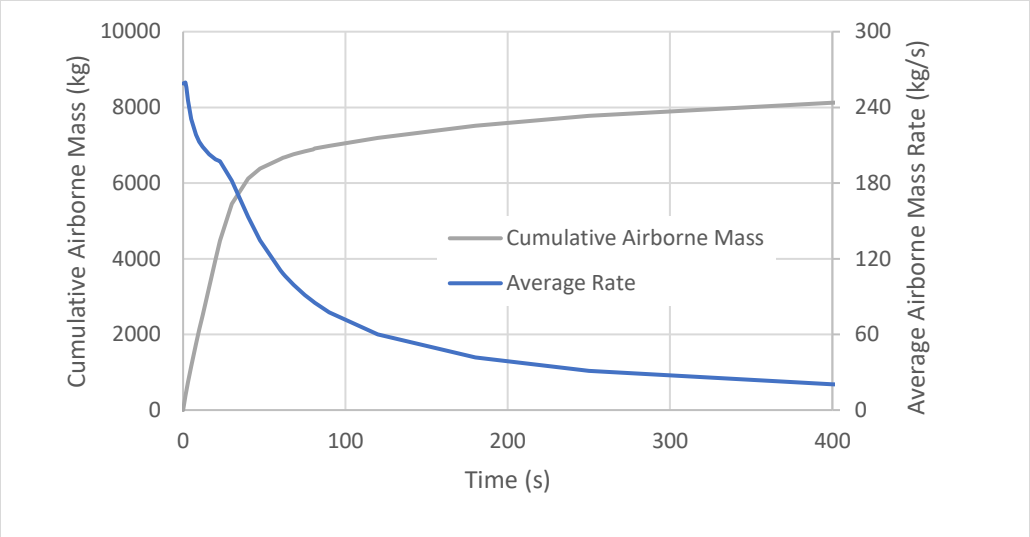

Figure 6. Cumulative airborne mass and average airborne rate as a function of time for Trial 7

Table 3. Cumulative mass fate and average airborne mass rate as a function of time for Trial 1.

Time, t (s)	Mass Released by t (kg)	Mass Deposited by t (kg)	Mass Airborne from Primary Release by t (kg)	Mass Evaporated by t (kg)	Average Vapor Fraction	Average Airborne Mass Rate (kg/s)
13.5 (t_x)	3021	1070	1951	583	0.434	188
20	3962	1403	2558	720	0.426	164
30	4411	1563	2848	890	0.440	125
36.6 (t_d)	4494	1591	2903	981	0.450	106
50.3	4545	1591	2954	1127	0.477	81.1
60	4545	1591	2954	1204	0.487	69.3

Table 4. Cumulative mass fate and average airborne mass rate as a function of time for Trial 7.

Time, t (s)	Mass Released by t (kg)	Mass Deposited by t (kg)	Mass Airborne from Primary Release by t (kg)	Mass Evaporated by t (kg)	Average Vapor Fraction	Average Airborne Mass Rate (kg/s)
20	5180	1926	3254	723	0.406	199
22.7 (t_x)	5897	2192	3705	772	0.399	197
30	7264	2701	4564	891	0.3923	182
60	8548	3175	5373	1265	0.412	111
61.6 (t_d)	8559	3175	5383	1281	0.413	108
81.1	8626	3175	5451	1462	0.436	85.2

Table 5 contains a set of inputs for the source specification necessary to run the atmospheric dispersion models for the JRII trials 1, 6 and 7. (All trials are planned to be modeled in the future.) The entries in Table 5 labeled "Primary release" are parameters which describe the release from primary containment as a jet and includes the portion of the liquid phase which rained out. In these entries, the release rate was estimated from experimental data, and the release duration was calculated to account for all of the mass released in a test. The entries labeled "Primary release modified for rainout" are parameters calculated by subtracting the mass rained out from the primary release mass, and the release duration was calculated to account for all of the mass released in a test that did not rain out. The entries labeled "Evaporated rainout" are parameters that account for the mass of chlorine that evaporates from the liquid that has rained out. The evaporation rate is averaged over (roughly) the duration of the "Primary release" source and assumed to apply until all of the rained out mass has evaporated. The area for the evaporated rainout is assumed to be the concrete pad area, but the liquid coverage of the concrete pad varied over time. Vapor densities were calculated assuming ideal gas behavior. As discussed above, all chlorine fluid properties are taken from the DIPPR database with the exception of liquid heat capacity which was based on data from Chlorine Institute Pamphlet 72. All parameters are reported after any depressurization process is complete.

Table 5. Averaged source emission rates and parameters.

	Trial 1	**Trial 6**	**Trial 7**
Primary release			
Discharge rate (kg/s)	224.	260.	259
Discharge period (s)	20.3	32.2	33.3
Temperature (ºC)	-37.3	-37.4	-37.4
Vapor fraction (ignoring KE effects)	0.171	0.172	0.172
Density (kg/m^3)	18.32	18.15	18.12
Velocity (m/s)	50.8	44.2	44.2
Area (m^2)	0.241	0.324	0.323
Primary release modified for rainout			
Discharge rate (kg/s)	145	168	162
Discharge period (s)	20.4	32.4	33.6
Temperature (ºC)	-37.3	-37.4	-37.4
Vapor fraction (ignoring KE effects)	0.264	0.266	0.274
Density (kg/m^3)	11.89	11.79	11.41
Velocity (m/s)	50.8	44.2	44.2
Area (m^2)	0.240	0.323	0.322
Evaporated rainout			
Discharge rate (kg/s)	43.2	34.0	34.0
Discharge period (s)	36.8	86.4	93.4
Temperature (ºC)	-37.3	-37.4	-37.4
Vapor fraction	1	1	1
Density (kg/m^3)	3.160	3.152	3.144
Area (m^2)	491	491	491

Conclusions

Sponsored by the U.S. Department of Homeland Security, the Defense Threat Reduction Agency (DTRA) of the U.S. Department of Defense, and Transport Canada, the Jack Rabbit II tests were designed to release liquid chlorine at ambient temperature in quantities of 5 to 20 T for the purpose of quantifying the behavior and hazards of catastrophic chlorine releases at scales represented by rail and truck transport vessels.

There are ongoing efforts to analyze data from the test program. One aspect of this analysis involves comparison of selected tests with predictions using available atmospheric dispersion models. For this comparison between atmospheric dispersion models to be most meaningful, it was desired to have a common set of model inputs including meteorological parameters and source parameters. This paper presents representative source parameters that can be applied in many different atmospheric dispersion models.

Acknowledgements

This field test program was sponsored by the Chemical Security Analysis Center (CSAC) of the U.S. Department of Homeland Security (DHS), the Defense Threat Reduction Agency (DTRA) of the U.S. Department of Defense, Transport Canada, and Defence Research and Development Canada (DRDC). In addition to the program's Dissemination and Near Source Working Group, we acknowledge the contribution of many people who planned and conducted the tests: DHS CSAC including Adolfo Negron and Shannon Fox; DTRA including Rick Fry; DPG including Damon Nicholson, Petr Serguievski, and Allison Hedrick; Chlorine Institute including Frank Reiner, Robyn Brooks, Therese Cirone, and Henry Ward; and the JR II Scientific Advisory Group (SAG) including Leo Stockham, Joe Chang, Steve Hanna, Allison Hedrick, Mike Sohn, and Thomas O. Spicer, III.

References

J.R. Couper, W.R. Penney, J.R. Fair, and S.M. Walas, "Chemical Process Equipment: Selection and Design," Elsevier, 2nd, 2005.

Spicer, T., and D. Miller, "Quantifying the Mass Discharge Rate of Flashing Two Phase Releases through Simple Holes to the Atmosphere," Process Safety Progress, 2018.

Spicer, T., A. Feuvrier, and S.B. Fox, "Transient Large-Scale Chlorine Releases in the Jack Rabbit II Field Tests: Rainout Source Data Analysis from Video Records," submitted to Journal of Loss Prevention in the Process Industries, 2018.